SMASIS2025-167868

PHYSICAL RESERVOIR COMPUTING WITH COMPLIANT FIBER NETWORKS

**Apoorva Khairnar[1], Yogesh Phalak[1], Jun Wang[1], Ziyang Zhou[1], Johannes Rümmelein[1],
Benjamin Jantzen[2], Suyi Li[1], Noel Naughton[1]**

[1]Department of Mechanical Engineering, Virginia Tech, Blacksburg, VA
[2]Department of Philosophy, Virginia Tech, Blacksburg, VA

ABSTRACT

Inspired by the webs of orb-weaving spiders, we explore the potential of compliant fiber networks to serve as mechanically intelligent physical reservoir computers. By exploiting the nonlinear dynamics inherent in the mechanical deformations of networks of connected fibers, we perform complex computational tasks without the need for conventional neural network architectures. Using Cosserat rod-based models, we simulate the behavior of these fiber networks, evaluating their computational abilities through the metrics of nonlinear capacity and memory capacity. We find that increasing the number of fibers enhances the nonlinear computational and memory recall capacity of the network, improving its computational performance. To validate these findings, we construct a physical prototype of the fiber network and experimentally demonstrate its ability to nonlinearly process input signals and recall previous inputs. Results suggest that compliant fiber networks can serve as effective physical reservoirs for mechano-intelligent computation, offering a low-cost, scalable, and manufacturable platform for applications in robotics, autonomous systems, and structural monitoring.

Keywords: Physical reservoir computing, Mechanical intelligence, Soft sensors, Cosserat rod, Fiber network

1. INTRODUCTION

Physical reservoir computing is an emerging computational framework that leverages the nonlinear dynamic properties of physical systems to perform complex computations [1], with particular recent attention paid to compliant mechanical systems [2–8]. Such systems can exhibit 'mechanically intelligent' behavior where taxing computational tasks are offloaded to its nonlinear physical dynamics [9, 10], serving to in turn simplify certain sensing and control tasks. Such physical intelligence is ubiquitous in nature, with biological systems regularly exploiting this emergent computational ability [11]. For example, orb-weaving spiders build webs made of crossing flexible fibers to capture prey. A spider can then extract information about its environment by sensing vibrations that travel along the web, enabling it to localize prey location, identify structural damage, and distinguish between different types of web deformation (e.g., prey vs wind) [12–15]. Inspired by this unique structure, here we evaluate the computational power of a network of crossing flexible fibers through the framework of physical reservoir computing.

Physical reservoir computing [1, 16, 17] extends the traditional theory of reservoir computing [18–21] to capitalize on the intrinsic dynamics of various mechanical systems to emulate computational behaviors. Examples include nonlinear spring-mass networks capable of emulation and pattern generation tasks [22–28], architected materials that respond predictably to input stimuli [29–32], origami-based mechanical systems that extract complex information from its structural dynamics [2–4], and soft robotic systems that integrate sensing and actuation to process information [5–8, 33]. These systems exhibit the core properties required of an effective reservoir: high-dimensionality, nonlinearity, fading memory, and the separation property [1]. These traits ensure the system can map input streams into unique, distinguishable dynamic states, retain short-term memory of previous inputs, and generalize across different computational tasks. Overall, physical reservoirs provide a compelling and scalable pathway toward embedding computation into material and structural systems, laying the groundwork for new forms of distributed, embodied intelligence.

We then construct an experimental platform to validate our simulation results and demonstrate the practical feasibility of our approach. We experimentally demonstrate the ability of a fiber network to perform nonlinear computation on an input signal and explore the impact of varying system parameters of fiber tension force, fiber stiffness, and number of fibers.

Our findings indicate that a network of crossing, flexible fibers inspired by the webs of orb-weaving spiders exhibit computational capabilities, endowing it with the ability to serve as

a physically intelligent structure. The network's ability to process information positions it as a low-cost and easy to manufacture compliant sensing technology with potential applications in robotics, autonomous systems, and structural monitoring. Overall, this integration of physical reservoir computing with a network of flexible fibers offers a promising direction for future mechano-intelligent sensing and provides a foundation for further exploration and development of such advanced soft sensing technologies.

2. COMPUTING WITH PHYSICAL DYNAMICS

In this work, we adopt the framework of physical reservoir computing and apply it to a network of crossing, compliant fibers. We apply a mechanical deformation input $u(t)$ to the network and measure the x-y displacements of m locations on the fiber network as $\mathbf{x}(t) = \{x_i(t), y_i(t) \ \forall \ i \in 1...m\}$ where $x_i(t), y_i(t) :\mapsto \mathbb{R}$ and m is determined based on the number of fibers in the network (i.e., $\mathbf{x}(t)$ has $2m$ entries). In general, the input $u(t)$ may be any continuously varying function. However, to evaluate the physical reservoir computing performance of our fiber network, we restrict ourselves in this work to a cubic spline fit to interpolation points that are evenly spaced 0.2 seconds apart (5 Hz) and are independent and identically drawn from a uniform probability distribution. This approach ensures that any structure observed in the output arises from the reservoir itself rather than from correlations in the input [34] while ensuring a continuous, smooth signal compatible with the elastic dynamics of the fiber network. Reservoir computers are universal filters [21] so that, for an arbitrary, real-valued nonlinear functional $z[u(t)]$, there exists a mapping, $\mathcal{W} : \mathbf{x}(t) \mapsto z[u(t)]$, such that $\mathcal{W}$ is linear in $\mathbf{x}(t)$. An approximation of such a map,

$$\hat{z}(t) = \mathbf{W} \cdot \mathbf{x}(t) \tag{1}$$

can be identified by estimating the linear weights $\mathbf{W} \in \mathbb{R}^{2m}$ through ridge regression.

In practice, the types of functions that can be learned are limited by the dynamics of particular reservoir. Our goal then is to probe the capability of a fiber network to serve as a physical reservoir computer. To do so, we first define a general capacity metric that captures the reservoir's ability to accurately learn a linear map $\mathbf{W}$ that provides an approximation $\hat{z}(t) = \mathbf{W} \cdot \mathbf{x}(t)$ of the functional $z[u(t)]$ over the time interval $[a, b]$ [34]

$$c[z] = 1 - \frac{\int_{t=a}^{b} (\hat{z}(t) - z[u(t)])^2 dt}{\int_{t=a}^{b} (z[u(t)] - \bar{z})^2 dt} \tag{2}$$

where $\bar{z}$ is the mean of $z[u(t)]$ over the time interval $[a, b]$. Based on this metric, we then define two specific metrics that quantify the computational capability of the reservoir: nonlinear capacity and memory capacity.

Nonlinear capacity measures the reservoir's ability to perform nonlinear computations on the current input $u(t)$ into the network. Here, we consider the ability of the reservoir to learn Legendre polynomials $P_k(u(t))$ of order k, such that $z_k[u(t)] = P_k(u(t))$ for $k \in \{1, ...N\}$ and $N = 10$. Legendre polynomials provide a complete and orthogonal basis set that
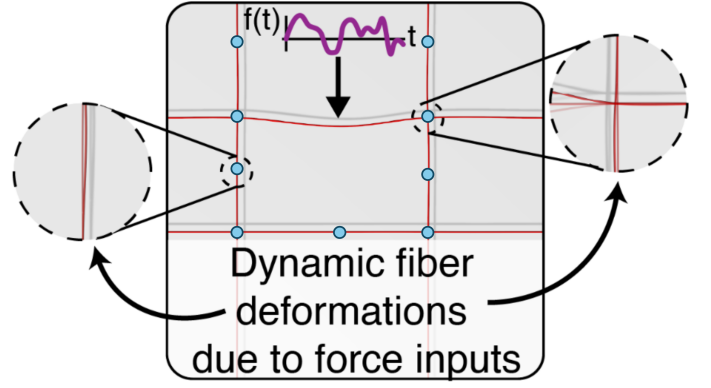

Figure 1: Snapshot of Cosserat rod-based fiber network actuated by a time-varying input force. The displacement of fiber nodes and midpoints (marked by blue dots) are tracked and used to generate compute mappings.

spans the interval $[-1, 1]$ and so provide not only a challenging test of the fiber network's nonlinear capability, but also indicate the ability of the reservoir to approximate any smooth function over this interval due to the efficiency with which Legendre polynomials represent such functions. We additionally define an overall nonlinear capacity of the reservoir as the sum of the individual capacity metrics $C_{nl} = 1/N \sum_{k=1}^{N} c[z_k]$.

Memory capacity measures the reservoir's ability to generate linear mappings that recall previous inputs. In this case, $z_\tau[u(t)] = u(t - \tau)$ where $\tau \in [0, T]$ is a time lag. We consider recall up to one second in the past ($T = 1.0$ s). Finally, we define the overall memory capacity of the reservoir as the integration of the individual capacity metrics over the recall interval $C_m = 1/T \int_{\tau=0}^{T} c[z_\tau]$.

3. FIBER NETWORK SIMULATIONS

We model the fiber network as an assembly of Cosserat rods, which are slender, one-dimensional elastic structures that can undergo all modes of deformation: bending, twisting, stretching, and shearing. The numerical implementation of Cosserat rods is computationally efficient as they accurately capture large 3D deformations through a one-dimensional representation, alleviating time-consuming remeshing difficulties and compute costs of 3D elasticity. In this study, we used Elastica [35], which is an open-source, Python-based implementation of a Cosserat rod numerical scheme whose utility in modeling fibrous dynamics has been demonstrated in a range of settings, from animal locomotion and manipulation [36–39] to fibrous metamaterials [40], and soft robotic design and control [41–44].

3.1. Simulation setup

To assemble a fiber network, we arrange individual rods in an evenly spaced $n \times n$ network where $n \in \{2, 3, 4, 6, 8, 10\}$ is the number of fibers. Fibers are fused together at intersection points using using a zero-displacement spring-damper boundary condition [37]. Fibers are fixed on one end and a constant tension force of F_t is applied axially on the other end to apply a pretension. Material parameters of the fibers are defined in Table 1. The
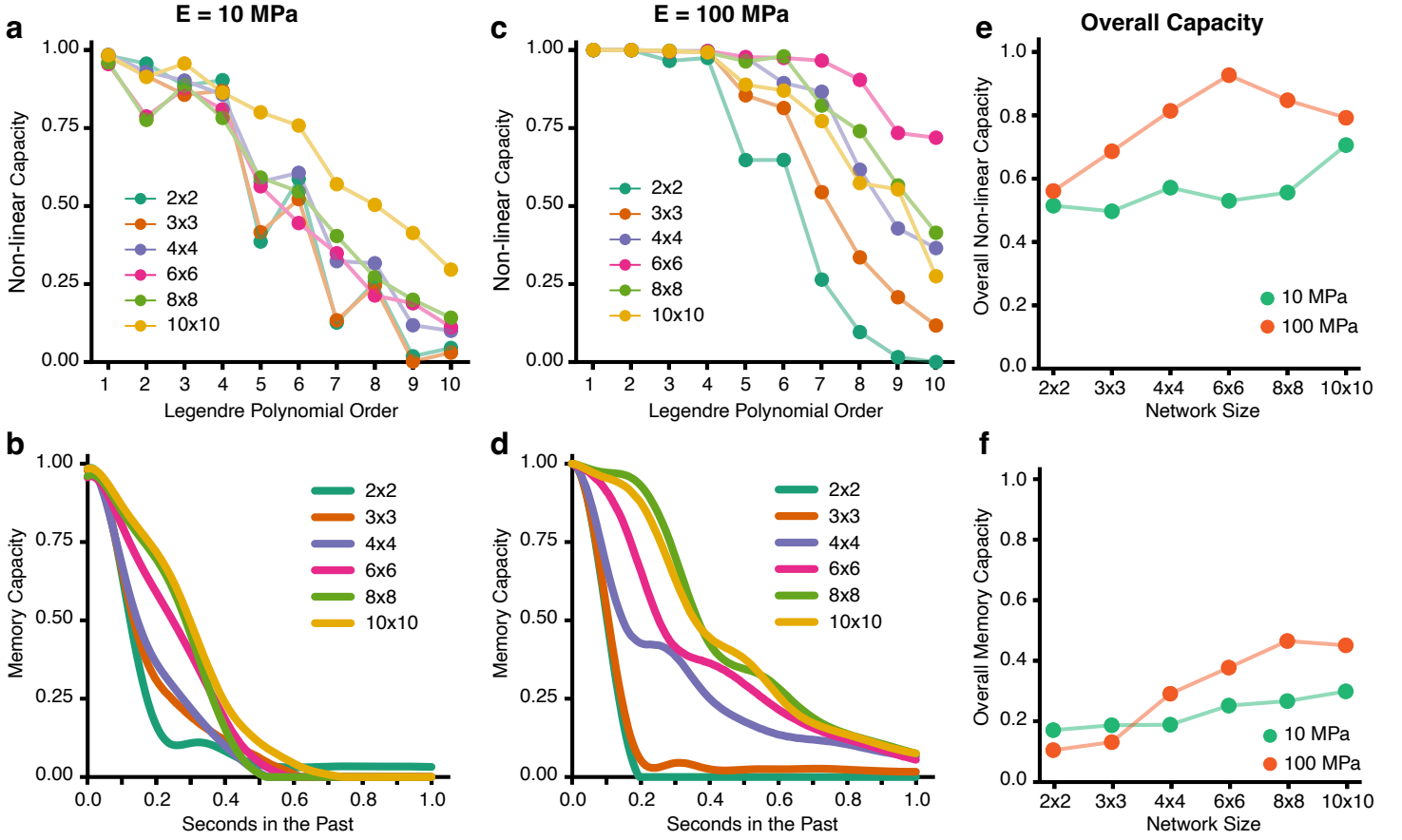
Figure 2: Network simulation results. **(a)** Nonlinear and **(b)** memory capacities of increasing network sizes for fibers with a Young's modulus of 10 MPa. **(c)** Nonlinear and **(d)** memory capacities of increasing network sizes for fibers with a Young's modulus of 100 MPa. Overall **(e)** nonlinear and **(f)** memory capacity of the networks. Larger networks and stiffer fibers tend to perform better. A different range of capacities are considered for (e) and (f) making their relative magnitudes not comparable.

architecture of a 2×2 network is shown in Figure 1. A similar architecture is used for larger fiber networks. For increasing number of fibers, the overall length of the network was held constant, with the spacing between parallel fibers being decreased to accommodate additional fibers. This decreases the effective aspect-ratio of fibers between fiber crossings, causing the overall response of larger fiber networks to be mechanically stiffer.

A time-varying external force $F_{ex}(t)$ is applied to the midpoint of the middle horizontal fiber to actuate the network. This force is a cubic spline that fits randomly generated timestamps in the interval $(0, T)$, where T is the duration of the simulation. For each fiber network setup, 40 simulations of 15 seconds each were run with a different F_{ex} used for each case. The maximum magnitude of F_{ex} was varied as 0.02 N, 0.04 N, 0.06 N, 0.2 N, 0.5 N and 1 N across $n \in \{2, 3, 4, 6, 8, 10\}$, respectively. The maximum force magnitude was empirically tuned to achieve consistent displacement of the actuation point across all network sizes. Simulation data was sampled at a 250 Hz frequency and the x-y displacements of fiber intersection points and the midpoints of fibers between intersections was recorded and used as the state of the physical reservoir $\mathbf{x}(t) \in \mathbb{R}^{2m}$. These inputs and outputs are then used with the physical reservoir computing framework described above to compute capacity metrics.

Table 1: Physical parameters of simulated fibers

Parameter	Value
Fiber Length	500 mm
Fiber Diameter	2 mm
Density	1000 kg/mm^3
Young's Modulus	10 MPa; 100 MPa
Tension Force (F_t)	0.01 N
Maximum External Force	0.02–1 N

We denote our desired output as $z(t)$ which is derived from our input to the reservoir $u(t) = F_{ex}(t)$. For evaluating the nonlinearity of the reservoir, our desired output is the Legendre Polynomial of order $k \in \{1, ..., 10\}$ and for memory evaluation it is the input from $\tau \in [0, 1]$ seconds in the past. We split $\mathbf{x}(t)$ and $z(t)$ into training and testing sets with a train to test ratio of 0.75:0.25. The training set is used to perform Ridge regression and obtain the mapping $\mathcal{W}$. We then use this mapping to estimate $\hat{z}(t)$ on the testing set and compute the capacity metrics as described in Section 2.

Table 2: Physical parameters of experimental setup

Parameter	Fishing Line (no pretension)	Fishing Line (pretension)	Elastic Cord (no pretension)	Elastic Cord (pretension)
Length	520 mm	490 mm	420 mm	490 mm
Diameter	0.45 mm	0.45 mm	4.79 mm	4.79 mm
Young's Modulus	1 GPa	1 GPa	22.8 MPa	22.8 MPa
Tension Force	0.47 N	2.26 N	0.47 N	2.26 N
Number of Fibers	2, 4, 6	2	2	2

3.2. Simulation results

We considered fiber networks with Young's moduli (E) of 10 MPa and 100 MPa. For each modulus, we varied the number of fibers in the network, testing network configurations of increasing number of fibers. For each fiber network, the nonlinear capacity of the network to compute Legendre polynomials $P_k(u(t))$ of order $k \in \{1...10\}$ and the memory capacity to remember inputs up to one second in the past was computed. Results for all simulations are shown in Figure 2.

The nonlinear capacities of networks with a Young's modulus of 10 MPa are shown in Fig. 2a and those with a modulus 100 MPa are shown in Fig. 2c. As expected, the nonlinear capacity of all networks decays as it is challenged to compute higher-order Legendre polynomials. For both moduli, larger networks generally exhibit higher capacity, as shown in Fig. 2e, where the sum of the capacities for all Legendre polynomial orders is plotted. Overall, stiffer 100 MPa networks outperformed softer 10 MPa network for all sizes. While the overall capacity of the 10 MPa networks gradually increased for increasing network size, the 100 MPa networks exhibit a much faster increase in overall capacity up to a size of 6×6 before a moderate drop off in overall capacity occurs. While the source of this decrease is unknown, it may indicate a limit to the improvement in computing capacity possible by simply increasing the network size.

Similar to the nonlinear capacity results, the memory capacities of networks with a Young's modulus of 10 MPa are shown in Fig. 2b and those with a modulus of 100 MPa are shown in Fig. 2d. We compute the ability of the fiber network to recall inputs $u(t - \tau)$ for $\tau \in [0, 1]$ seconds, leading to a continuous distribution of capacities compared to the discrete set of results based on polynomial order for the nonlinear capacity. For both 10 MPa and 100 MPa fibers, larger networks exhibited improved memory capacity, with better recall of inputs further in the past. For 2×2 and 3×3 networks, the 10 MPa fiber network outperformed the 100 MPa fiber network in their overall memory capacity (Fig. 2f). However, as with nonlinear capacity, the 100 MPa fiber networks exhibit faster improvement in their overall memory as the network size increases compared to the more moderate rate of increase for 10 MPa. As a result, the 100 MPa outperforms the 10 MPa networks for fiber sizes larger than 4×4. The overall memory capacity of the 100 MPa networks peaks at 8×8 before leveling off for 10×10, again possibly indicating a limit on the amount of improved performance available from simply increasing the size of a fiber network.

Overall, these simulation result indicate that crossing fiber networks made of slender, flexible fibers can be used to perform nonlinear computations and process information with the performance of the network strongly impacted by both the fiber's material properties and network architecture, necessitating careful setup of the network.

4. EXPERIMENTAL VALIDATION

We next validate the findings of our simulations by performing experiments using fiber networks to examine their capacity for physical reservoir computing. We first consider a 2×2 network under different material and boundary conditions to identify a suitable physical reservoir setup and then explore the impact of increasing the number of fibers on the computational capability of the fiber network.

4.1. Experimental setup

Our experimental setup consists of a fiber network organized in an evenly spaced $n \times n$ grid. One end of each fiber is fixed while the other is connected to springs ($k = 52.5$ N/m) to maintain consistent tension (Fig. 3). The fibers are bonded at fiber crossings using a Silicone Rubber adhesive (Sil-Poxy). To monitor the state of the reservoir $\mathbf{x}(t)$, red markers are attached at fiber intersections and midpoints between them and tracked using video recording. The fiber network is actuated at the midpoint of the
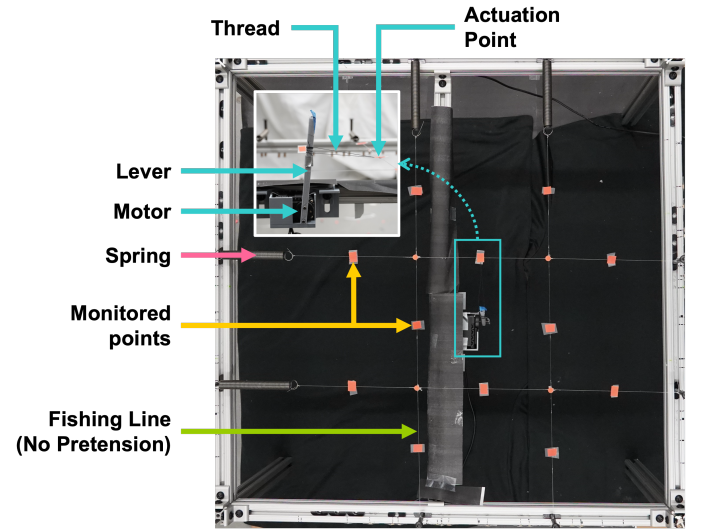

Figure 3: Experimental setup of 2×2 **network.** A servomotor with a lever arm attached to the fiber network by a string actuates the fiber network while the x-y position of the red tracking points is recorded via a camera positioned above the network.
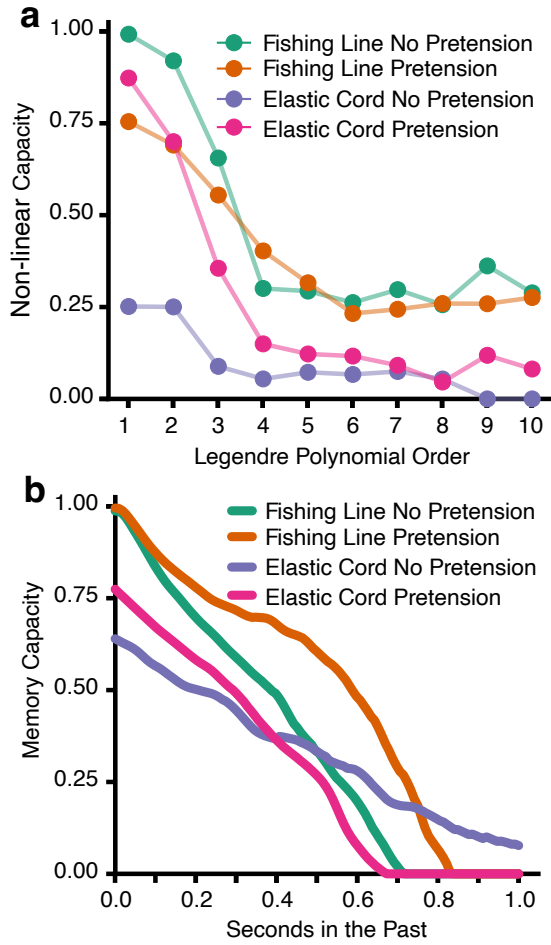
Figure 4: 2×2 network experimental results. (a) Nonlinear and **(b)** memory capacity of networks with different fiber materials and tension levels. A network made of fishing line and no pretension performed best overall.

Figure 5: Impact of network size on physical reservoir's **(a)** nonlinear and **(b)** memory capacity. While the 4×4 network outperforms the 2×2 network in both metrics, the 6×6 network only outperforms smaller networks in its nonlinear capacity while exhibiting a decrease in memory capacity relative to smaller networks.

central horizontal fiber using a Dynamixel AX-18A servo motor. A thread connects the motor's lever to the fiber (Fig. 3 inset), allowing controlled actuation. A time-varying input is created by modulating the joint angle of the motor using a cubic spline fitted to randomly chosen timestamps over the experiment duration.

Experiments were run under different network conditions by changing the fiber material, pretension, and network size. The parameters used for each setup are summarized in Table 2. Each experiment was conducted for either 30 or 60 seconds and recorded at 120 FPS in HD (1920×1080) using a Sony α7 III mirrorless camera. The frames extracted from the video are segmented to track the displacement of each marker over time. We apply K-means Clustering to label marker positions, and convert their coordinates from pixels to millimeters. For these experiments, we use the normal displacement of the actuation point as the input $u(t) = y(t)$ (compared to the force value $F_{ex}(t)$ used in simulations). As with simulations, the x-y displacement of all other points is tracked and used as the output $\mathbf{x}(t)$ of the physical reservoir to determine computing capacity metrics.
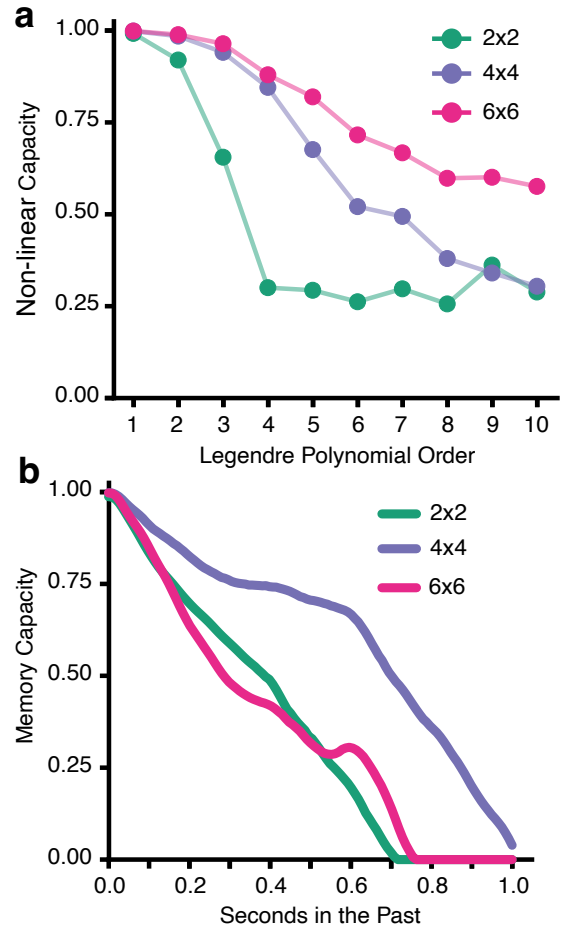
4.2. 2×2 fiber network results

We first examine a 2×2 network to study the effect of fiber material and pretension on the reservoir performance (Fig. 4). Pretension was introduced by manually shortening the fibers, stretching the springs closer to their maximum extension. We tested two materials - monofilament fishing line ($E \approx 1$ GPa) and elastic bungee cord ($E \approx 22.8$ MPa), each under pretensioned and non-pretensioned conditions, resulting in four configurations. Young's moduli were approximated by conducting a manual force-displacement measurement.

Both non-linear capacity for increasing Legendre polynomial order (Fig. 4a) and memory capacity (Fig. 4b) was computed for all four networks. Overall, fiber networks made of fishing line without pretensioning demonstrated the highest nonlinear processing ability while the fiber network made of fishing line with pretensioning exhibited the largest memory capacity.

In all four cases, the nonlinear capacity decreased rapidly beyond Legendre polynomials of degree 2, asymptotically approaching zero at higher orders. Memory capacity similarly decayed as the input delay time increased. Both results are broadly
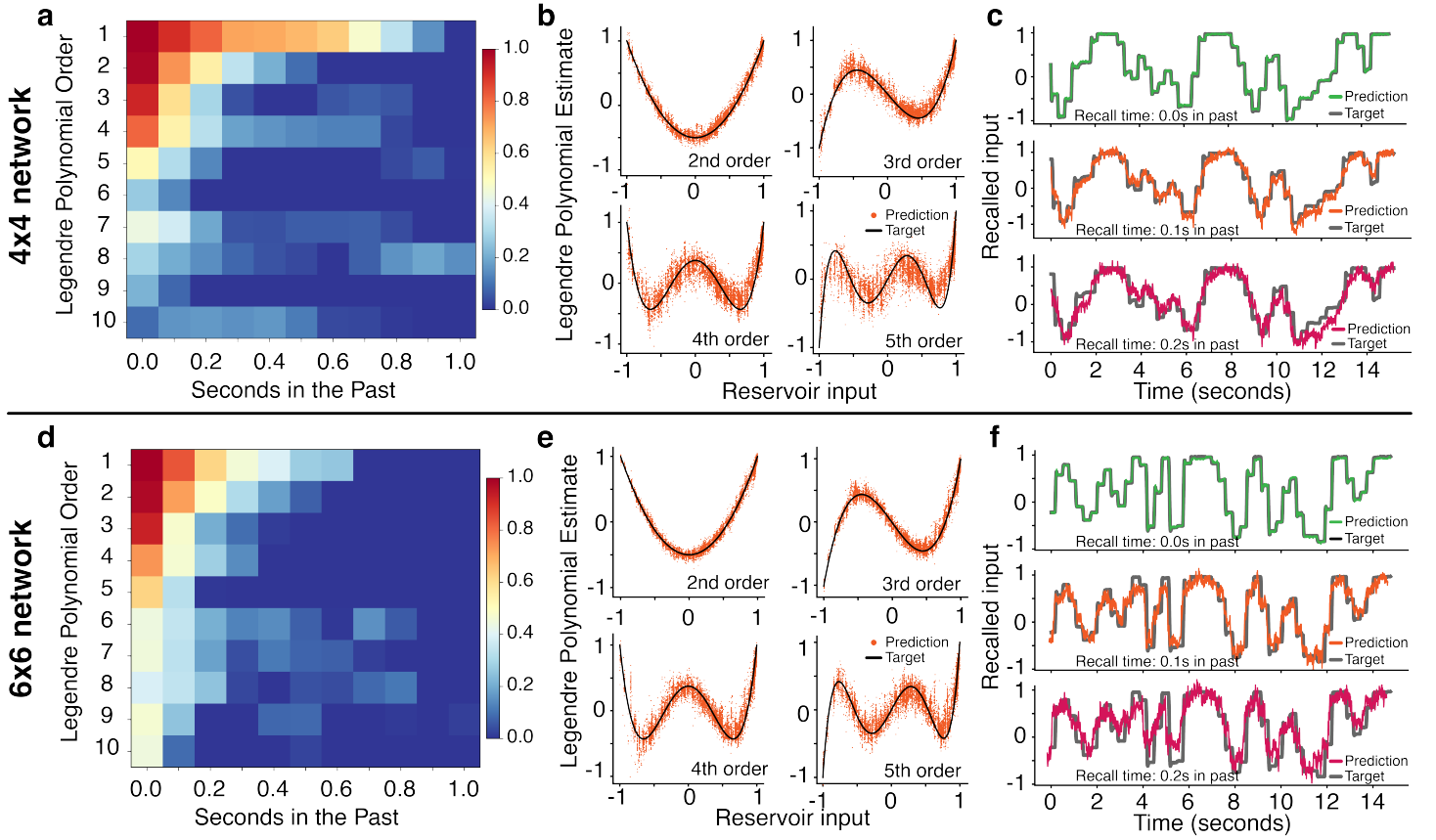
Figure 6: Reservoir performance of 4×4 and 6×6 networks. Performance of a 4×4 fiber network: **(a)** Combined nonlinear and memory capacity metrics of the network (top row and left column correspond to the results shown in Figure 5). Color denotes the capacity metric of the fiber network to compute a polynomial of degree $k \in \{1, ...10\}$ for the input from $\tau \in \{0.0, 0.1, ...1.0\}$ seconds in the past. **(b)** Performance of the reservoir at transforming the current input into its second- through fifth-order Legendre polynomial output. Dark line is desired output value. **(c)** Performance of reservoir's memory recall performance, recalling the input into the reservoir from 0.0 seconds (i.e. current input), 0.1 seconds, and 0.2 seconds in the past. Dark line is true input value from that previous time point. Performance of a 6×6 fiber network: **(d)** Combined capacity metrics of the network, **(e)** nonlinear performance of Legendre polynomials, and **(f)** memory recall performance.

in keeping with the simulation results. Further, networks made of the stiffer fishing line material substantially outperformed fiber networks made of the softer elastic cord, a result also in keeping with the simulation results of fibers with Young's moduli of 100 MPa outperforming networks with fibers of 10 MPa. This performance difference likely arises from the increased mechanical stability in stiffer fiber networks. In contrast, softer networks exhibit greater nonlinearity in their mechanical response, leading to more chaotic and less consistent behavior, thus limiting computational performance. Higher levels of slipping between fibers were also observed in the experiments on softer configurations, further contributing to noise in the network's response. Notably, applying pretension to the softer fibers appeared to partially offset these effects, as seen in the improved performance of the elastic cord under pretension. These results suggest it may be possible to maximize the computational performance of the fiber network reservoir by tuning its dynamical response to inputs through careful matching of the input force dynamics with the fiber material properties (stiffness) and pretension on the network.

4.3. Scaling fiber network size

We next scaled the fiber network size, considering both 4×4 and 6×6 networks (Fig. 5). Based on the results for the 2×2 network, fishing line without pretension was chosen as the network setup for all experiments due to its overall performance in both non-linear and memory capacity tests.

Nonlinear capacity increases substantially as the network size increases (Fig. 5a) with a more gradual decay of capacity exhibited by larger fiber networks as the polynomial degree increases. Additionally, Table 3 reports the capacity, R^2-score and Root Mean Squared Error (RMSE) of the three network configurations for a Legendre Polynomial of degree 4. As the network size increases, the capacity and R^2-score for nonlinearity increases while the RMSE decreases. This trend indicates increasing computational capability of networks with more fibers, and so, more complex dynamic interactions of the fibers. This is in keeping with similar observations from the simulations and also consistent with the notion that systems with more complex physical dynamics have better reservoir computing properties.

The performance change of larger fiber networks in terms

Table 3: Quantitative comparison of network performance

Network Size	4th-order Legendre			Recall 0.2s in past		
	Capacity	R^2	RMSE	Capacity	R^2	RMSE
2×2	0.301	0.289	0.323	0.684	0.620	0.299
4×4	0.845	0.847	0.165	0.816	0.826	0.253
6×6	0.880	0.882	0.131	0.619	0.655	0.342

of their memory capacity is less clear with the overall memory capacity (the sum of the memory capacities for all time points in past) of the 4×4 network (71.650) outperforming the 2×2 network (41.43), but the 6×6 network (41.16) exhibiting degraded performance, with memory capacity on par with the 2×2 network (Fig. 5b). Table 3 reports the memory capacity, R^2-score, and RMSE of the three network sizes when tasked with recalling the input 0.2 seconds in the past. The memory capacities and R^2-scores of the 2×2 and 6×6 networks are quite close whereas the capacity and R^2-scores of 4×4 network are comparatively higher as well as having the lowest RMSE. This is in contrast to the simulation results which showed monotonic increases in memory capacity as the network size increased. The source of this disagreement is unknown, though experimental difficulties of setting up the larger 6×6 network may play a role.

Finally, we explore the performance of the 4×4 and 6×6 networks (Fig. 6). In Fig 6a,d, we merge our non-linear and memory capacities to consider the ability of the reservoir to perform non-linear computation on past inputs ($z[u(t)] = P_k(u - \tau)$ in Eq. 2). The depicted heatmaps show the capacity of the fiber network to compute a polynomial of degree $k \in \{1, ...10\}$ for the input from $\tau \in \{0.0, 0.1, ...1.0\}$ seconds in the past. For reference, the left-most column and top-most row correspond to the previously described nonlinear capacity and memory capacity metrics, respectively.

The results of Fig. 6a,d suggest a possible tradeoff between the non-linear and memory capacity of our physical reservoir, a result in line with reservoir computing theory [34, 45]. The 6×6 network is more oriented towards non-linear computation, as indicated by the more vertical organization of Fig. 6d. In contrast, the more horizontal organization of the 4×4 network's heatmap in Fig. 6a suggests an orientation towards memory tasks.

This tradeoff is confirmed by examining the performance of the respective reservoirs. In Fig. 6b,e, reservoir predictions of Legendre polynomials for degree 2–5 are shown for the 4×4 and 6×6 networks, respectively. While both networks perform very well for lower order polynomials, for polynomials of order 4 and greater, the spread of points for the 6×6 network are notably more compact and conforming to the true value than the 4×4 network.

Similarly, the 4×4 network exhibits better memory recall than the 6×6 network as demonstrated in Fig. 6c,f, where the ability of a fiber network to recall the current input as well as inputs from 0.1 and 0.2 seconds in the past is plotted. The 4×4 network is better able to recall the full range of input, especially for inputs from 0.2 seconds in the past while the 6×6 network struggles to accurately recall larger inputs magnitude from this far back.

5. CONCLUSION

Inspired by orb-weaving spider webs, in this work we explored the computational potential of networks composed of crossing flexible fibers within the framework of physical reservoir computing. Through simulations and physical experiments, we demonstrated that these networks are capable of performing nonlinear computations and retain short-term memory—two key traits of reservoir computing. We showed how material properties, pretension, and network size influence the computational behavior, potentially allowing for tunable performance based on task demands.

Overall, this study confirms that such crossing fiber networks can serve as physically intelligent structures that sense and process mechanical information inherently via their dynamics. This ability portends exciting opportunities for the design of low-cost and easy to make fibrous sensing elements with potential applications in robotics, autonomous systems, and structural health monitoring. As the field of mechano-intelligent materials continues to grow, this work demonstrates how simple, soft architectures of compliant materials can be harnessed for embedded computation and advancing the integration of sensing and computing in physical form.

REFERENCES

[1] Tanaka, Gouhei, Yamane, Toshiyuki, Héroux, Jean Benoit, Nakane, Ryosho, et al. "Recent advances in physical reservoir computing: A review." *Neural Networks* Vol. 115 (2019): pp. 100–123.

[2] Bhovad, Priyanka and Li, Suyi. "Physical reservoir computing with origami and its application to robotic crawling." *Scientific Reports* Vol. 11 No. 1 (2021): p. 13002.

[3] Liu, Zuolin, Fang, Hongbin, Xu, Jian, and Wang, Kon-Well. "Discriminative transition sequences of origami metamaterials for mechanologic." *Advanced Intelligent Systems* Vol. 5 No. 1 (2023): p. 2200146.

[4] Wang, Jun and Li, Suyi. "Building intelligence in the mechanical domain—Harvesting the reservoir computing power in origami to achieve information perception tasks." *Advanced Intelligent Systems* Vol. 5 No. 9 (2023): p. 2300086.

[5] Nakajima, Kohei, Hauser, Helmut, Kang, Rongjie, Guglielmino, Emanuele, et al. "A soft body as a reservoir: case studies in a dynamic model of octopus-inspired soft robotic arm." *Frontiers in computational neuroscience* Vol. 7 (2013): p. 91.

[6] Nakajima, Kohei, Li, Tao, Hauser, Helmut, and Pfeifer, Rolf. "Exploiting short-term memory in soft body dynamics as a computational resource." *Journal of The Royal Society Interface* Vol. 11 No. 100 (2014): p. 20140437.

[7] Nakajima, Kohei, Hauser, Helmut, Li, Tao, and Pfeifer, Rolf. "Exploiting the dynamics of soft materials for machine learning." *Soft robotics* Vol. 5 No. 3 (2018): pp. 339–347.

[8] Degrave, Jonas, Caluwaerts, Ken, Dambre, Joni, and Wyffels, Francis. "Developing an embodied gait on a compliant quadrupedal robot." *2015 IEEE/RSJ international conference on Intelligent Robots and Systems (IROS)*: pp. 4486–4491. 2015. IEEE.

[9] Ulrich, Nathan Thatcher. "Grasping with mechanical intelligence." Technical report no. 1988.

[10] Pfeifer, Rolf and Bongard, Josh. *How the body shapes the way we think: a new view of intelligence*. MIT press (2006).

[11] Wang, Tianyu, Pierce, Christopher, Kojouharov, Velin, Chong, Baxi, et al. "Mechanical intelligence simplifies control in terrestrial limbless locomotion." *Science Robotics* Vol. 8 No. 85 (2023): p. eadi2243.

[12] Wu, Jun, Miller, Thomas E, Cicirello, Alice, and Mortimer, Beth. "Spider dynamics under vertical vibration and its implications for biological vibration sensing." *Journal of the Royal Society Interface* Vol. 20 No. 206 (2023): p. 20230365.

[13] Landolfa, MA and Barth, FG. "Vibrations in the orb web of the spider Nephila clavipes: cues for discrimination and orientation." *Journal of Comparative Physiology A* Vol. 179 (1996): pp. 493–508.

[14] Mortimer, Beth. "A spider's vibration landscape: adaptations to promote vibrational information transfer in orb webs." *Integrative and Comparative Biology* Vol. 59 No. 6 (2019): pp. 1636–1645.

[15] Masters, W Mitch. "Vibrations in the orbwebs of Nuctenea sclopetaria (Araneidae) II. Prey and wind signals and the spider's response threshold." *Behavioral ecology and sociobiology* Vol. 15 (1984): pp. 217–223.

[16] Konkoli, Zoran, Nichele, Stefano, Dale, Matthew, and Stepney, Susan. "Reservoir computing with computational matter." *Computational matter* (2018): pp. 269–293.

[17] Nakajima, Kohei. "Physical reservoir computing—an introductory perspective." *Japanese Journal of Applied Physics* Vol. 59 No. 6 (2020): p. 060501.

[18] Jaeger, Herbert. "The "echo state" approach to analysing and training recurrent neural networks-with an erratum note." *Bonn, Germany: German national research center for information technology gmd technical report* Vol. 148 No. 34 (2001): p. 13.

[19] Maass, Wolfgang. "Liquid state machines: motivation, theory, and applications." *Computability in context: computation and logic in the real world* (2011): pp. 275–296.

[20] Schrauwen, Benjamin, Verstraeten, David, and Van Campenhout, Jan. "An overview of reservoir computing: theory, applications and implementations." *Proceedings of the 15th european symposium on artificial neural networks. p. 471-482 2007*: pp. 471–482. 2007.

[21] Nakajima, Kohei and Fischer, Ingo. *Reservoir computing*. Springer (2021).

[22] Hauser, Helmut, Ijspeert, Auke J, Füchslin, Rudolf M, Pfeifer, Rolf, and Maass, Wolfgang. "Towards a theoretical foundation for morphological computation with compliant bodies." *Biological cybernetics* Vol. 105 (2011): pp. 355–370.

[23] Hauser, Helmut, Ijspeert, Auke J, Füchslin, Rudolf M, Pfeifer, Rolf, and Maass, Wolfgang. "The role of feedback in morphological computation with compliant bodies." *Biological cybernetics* Vol. 106 (2012): pp. 595–613.

[24] Yamanaka, Yuki, Yaguchi, Takaharu, Nakajima, Kohei, and Hauser, Helmut. "Mass-spring damper array as a mechanical medium for computation." *International Conference on Artificial Neural Networks*: pp. 781–794. 2018. Springer.

[25] Urbain, Gabriel, Degrave, Jonas, Carette, Benonie, Dambre, Joni, and Wyffels, Francis. "Morphological properties of mass–spring networks for optimal locomotion learning." *Frontiers in neurorobotics* Vol. 11 (2017): p. 16.

[26] Dion, Guillaume, Mejaouri, Salim, and Sylvestre, Julien. "Reservoir computing with a single delay-coupled non-linear mechanical oscillator." *Journal of Applied Physics* Vol. 124 No. 15 (2018).

[27] Du, Chao, Cai, Fuxi, Zidan, Mohammed A, Ma, Wen, et al. "Reservoir computing using dynamic memristors for temporal information processing." *Nature communications* Vol. 8 No. 1 (2017): p. 2204.

[28] Yamane, Toshiyuki, Katayama, Yasunao, Nakane, Ryosho, Tanaka, Gouhei, and Nakano, Daiju. "Wave-based reservoir computing by synchronization of coupled oscillators." *Neural Information Processing: 22nd International Conference, ICONIP 2015, Istanbul, Turkey, November 9-12, 2015, Proceedings Part III 22*: pp. 198–205. 2015. Springer.

[29] Paul, Chandana. "Investigation of morphology and control in biped locomotion." Ph.D. Thesis, Verlag nicht ermittelbar. 2004.

[30] Paul, Chandana. "Morphological computation: A basis for the analysis of morphology and control requirements." *Robotics and Autonomous Systems* Vol. 54 No. 8 (2006): pp. 619–630.

[31] Caluwaerts, Ken and Schrauwen, Benjamin. "The body as a reservoir: locomotion and sensing with linear feedback." *2nd International conference on Morphological Computation (ICMC 2011)*. 2011.

[32] Zhang, Yuning and Wang, Kon-Well. "Harnessing physical reservoir computing in nonlinear mechanical metastructures." *AIAA Scitech 2022 Forum*: p. 1464. 2022.

[33] Li, Tao, Nakajima, Kohei, Cianchetti, Matteo, Laschi, Cecilia, and Pfeifer, Rolf. "Behavior switching using reservoir computing for a soft robotic arm." *2012 IEEE International Conference on Robotics and Automation*: pp. 4918–4924. 2012. IEEE.

[34] Dambre, Joni, Verstraeten, David, Schrauwen, Benjamin, and Massar, Serge. "Information processing capacity of dynamical systems." *Scientific reports* Vol. 2 No. 1 (2012): p. 514.

[35] Tekinalp, Arman, Kim, Seung Hyun, Bhosale, Yashraj, Parthasarathy, Tejaswin, et al. "PyElastica." (2023). DOI 10.5281/zenodo.7658872. URL https://doi.org/10.5281/zenodo.7658872.

[36] Gazzola, Mattia, Dudte, LH, McCormick, AG, and Mahadevan, Lakshminarayanan. "Forward and inverse problems in the mechanics of soft filaments." *Royal Society open science* Vol. 5 No. 6 (2018): p. 171628.

[37] Zhang, Xiaotian, Chan, Fan Kiat, Parthasarathy, Tejaswin, and Gazzola, Mattia. "Modeling and simulation of complex dynamic musculoskeletal architectures." *Nature communications* Vol. 10 No. 1 (2019): pp. 1–12.

[38] Zhang, Xiaotian, Naughton, Noel, Parthasarathy, Tejaswin, and Gazzola, Mattia. "Friction modulation in limbless, three-dimensional gaits and heterogeneous terrains." *Nature communications* Vol. 12 No. 1 (2021): p. 6076.

[39] Tekinalp, Arman, Naughton, Noel, Kim, Seung Hyun, Halder, Udit, et al. "Topology, dynamics, and control of a muscle-architected soft arm." *Proceedings of the National Academy of Sciences* Vol. 121 No. 41 (2024): p. e2318769121.

[40] Bhosale, Yashraj, Weiner, Nicholas, Butler, Alex, Kim, Seung Hyun, et al. "Micromechanical origin of plasticity and hysteresis in nestlike packings." *Physical review letters* Vol. 128 No. 19 (2022): p. 198003.

[41] Naughton, Noel, Sun, Jiarui, Tekinalp, Arman, Parthasarathy, Tejaswin, et al. "Elastica: A compliant mechanics environment for soft robotic control." *IEEE Robotics and Automation Letters* Vol. 6 No. 2 (2021): pp. 3389–3396.

[42] Chang, Heng-Sheng, Halder, Udit, Shih, Chia-Hsien, Naughton, Noel, et al. "Energy-shaping control of a muscular octopus arm moving in three dimensions." *Proceedings of the Royal Society A* Vol. 479 No. 2270 (2023): p. 20220593.

[43] Shih, Chia-Hsien, Naughton, Noel, Halder, Udit, Chang, Heng-Sheng, et al. "Hierarchical control and learning of a foraging cyberoctopus." *Advanced Intelligent Systems* Vol. 5 No. 9 (2023): p. 2300088.

[44] Naughton, Noel, Tekinalp, Arman, Shivam, Keshav, Kim, Seung Hung, et al. "Neural reservoir control of a soft biohybrid arm." *arXiv preprint arXiv:2503.09477* (2025).

[45] Dale, Matthew, Miller, Julian F, Stepney, Susan, and Trefzer, Martin A. "A substrate-independent framework to characterize reservoir computers." *Proceedings of the Royal Society A* Vol. 475 No. 2226 (2019): p. 20180723.